Cell Research (2016) 26:713-727.

www.nature.com/cr

ORIGINAL ARTICLE

# Reversing drug resistance of soft tumor-repopulating cells by tumor cell-derived chemotherapeutic microparticles

Jingwei Ma[1, 2, *], Yi Zhang[1, *], Ke Tang[1, 2], Huafeng Zhang[1], Xiaonan Yin[1], Yong Li[2], Pingwei Xu[3], Yanling Sun[2], Ruihua Ma[2], Tiantian Ji[2], Junwei Chen[3], Shuang Zhang[3], Tianzhen Zhang[1], Shunqun Luo[2], Yang Jin[4], Xiuli Luo[5], Chengyin Li[5], Hongwei Gong[5], Zhixiong Long[6], Jinzhi Lu[1], Zhuowei Hu[7], Xuetao Cao[1], Ning Wang[3, 8], Xiangliang Yang[9], Bo Huang[1, 2]

*[1]National Key Laboratory of Medical Molecular Biology & Department of Immunology, Institute of Basic Medical Sciences, Chinese Academy of Medical Sciences, Beijing 100005, China; [2]Department of Biochemistry & Molecular Biology, Tongji Medical College, Huazhong University of Science & Technology, Wuhan, Hubei 430030, China; [3]Laboratory for Cell Biomechanics and Regenerative Medicine, Department of Biomedical Engineering, School of Life Science and Technology, Huazhong University of Science and Technology, Wuhan, Hubei 430074, China; [4]Department of Respiratory and Critical Care Medicine, Key Laboratory of Pulmonary Diseases of Health Ministry, Union Hospital, Tongji Medical College, Huazhong University of Science and Technology, Wuhan, Hubei 430022, China; [5]Department of Oncology, Hubei Provincial Hospital of TCM, Wuhan, Hubei 430061, China; [6]Department of Oncology, the Fifth Hospital of Wuhan, Wuhan, Hubei 430050, China; [7]Molecular Immunology and Pharmacology Group, State Key Laboratory of Bioactive Substance and Function of Natural Medicines, Institute of Materia Medica, Chinese Academy of Medical Sciences & Peking Union Medical College, Beijing, China; [8]Department of Mechanical Science and Engineering, College of Engineering, University of Illinois at Urbana-Champaign, Urbana, IL 61801, USA; [9]National Engineering Research Center for Nanomedicine, College of Life Science and Technology, Huazhong University of Science and Technology, Wuhan, Hubei 430074, China*

**Developing novel approaches to reverse the drug resistance of tumor-repopulating cells (TRCs) or stem cell-like cancer cells is an urgent clinical need to improve outcomes of cancer patients. Here we show an innovative approach that reverses drug resistance of TRCs using tumor cell-derived microparticles (T-MPs) containing anti-tumor drugs. TRCs, by virtue of being more deformable than differentiated cancer cells, preferentially take up T-MPs that release anti-tumor drugs after entering cells, which in turn lead to death of TRCs. The underlying mechanisms include interfering with drug efflux and promoting nuclear entry of the drugs. Our findings demonstrate the importance of tumor cell softness in uptake of T-MPs and effectiveness of a novel approach in reversing drug resistance of TRCs with promising clinical applications.**

***Keywords*:** tumor-repopulating cells; drug-packaging microparticles; drug resistance; nuclear delivery
*Cell Research* (2016) **26**:713-727. doi:10.1038/cr.2016.53; published online 10 May 2016

## Introduction

Resistance to chemotherapeutic drugs is a leading cause of failure in cancer treatment. Stem cell-like cancer cells (SCLCCs) are a subset of cancer cells that can self-renew and are highly tumorigenic. SCLCCs are also regarded as the major contributor to drug resistance. Even though chemotherapy can kill a majority of cells inside tumor tissues, it is believed that SCLCCs are left behind, thus constituting a major mechanism of drug resistance [1]. Indeed, it has been reported that SCLCCs contribute to the resistance to various chemotherapeutic drugs such as cisplatin (Cis), paclitaxel (PTX), doxorubicin (DOX), imatinib, temozolomide, and etoposide in many different tumor types, including breast, colon, lung, liver, brain, pancreatic, ovarian, and prostate can-

*These two authors contributed equally to this work.
Correspondence: Bo Huang
E-mail: tjhuangbo@hotmail.com
Received 1 November 2015; revised 18 January 2016; accepted 17 February 2016; published online 10 May 2016

cers and leukemia [2-5]. Consistent with these findings, SCLCCs usually express high levels of anti-apoptotic proteins, DNA repair enzymes and ATP-binding cassette (ABC) transporters, which help SCLCCs survive the drug attack [6-8]. Thus, unraveling the roles of SCLCCs in tumorigenesis and drug resistance has changed our view on chemotherapy and aided the development of new therapeutic strategies against cancers [9-11]. Multiple signaling pathways, including WNT, TGF-β, Notch and Hedgehog pathways, have been found to play important roles in SCLCCs [12]. Interfering with these signaling pathways provide potential strategies for targeting SCLCCs. Meanwhile, altering the tumor microenvironment to destroy the niches for SCLCCs is an alternative strategy with great potential [13]. In addition, exploitation of the immune system may yield another dimension of anti-SCLCC therapy by directing specific T cells to recognize and attack SCLCCs [14]. However, due to heterogeneity and plasticity of SCLCCs, building carriers for currently available drugs and devising novel anti-SCLCC therapies remain an urgent need.

SCLCCs have been identified in a variety of tumor types using combinations of cell-surface markers, such as CD133, CD44, CD24 and CD90, or certain intracellular proteins such as aldehyde dehydrogenase 1 (ALDH1) [15]. However, identification of SCLCCs through these conventional methods that depend on stem cell markers is often unreliable, as these markers are often expressed by other cell types. We have recently developed a mechanics-based method to select and amplify a minor population of tumor cells by culturing single tumor cells in soft 3D fibrin gels [16]. The growing colonies showed spheroid-like morphology and were resistant to chemotherapeutic drugs. More significantly, when these spheroids were digested into single cells by dispase, as few as 10 cells were able to grow tumors in immunocompetent mice. We thus functionally defined these soft 3D fibrin gel-cultured cells as tumor-repopulating cells (TRCs) [16, 17]. These TRCs can be easily isolated from the spheroids formed in the soft fibrin gels. In this study we present a novel approach using anti-tumor drug-packaging tumor cell-derived microparticles (T-MPs) to reverse drug resistance of TRCs.

## Results

*Chemotherapeutic drug-packaging T-MPs target TRCs in cancer patients with malignant pleural effusion and reverse the drug resistance of TRCs in vitro*

In response to stimuli, cells may release membrane vesicles with 100-1 000 nm size [18]. These membrane vesicles, named as microparticles (MPs), can be taken up by normal or cancerous cells [19, 20]. We have recently developed a natural drug delivery system with T-MPs, which can efficiently kill tumor cells without adverse side effects [21]. These findings encouraged us to assess the efficacy of this delivery system in cancer patients. Six end-stage lung cancer patients with metastatic malignant pleural effusion were recruited. The primary tumor cells in the malignant fluids from patients were Cis-resistant and showed higher expression of multidrug resistance genes, compared with A549 tumor cell line (Supplementary information, Figure S1). Three patients were treated with intrathoracic injection of Cis-packaging MPs (Cis-MPs; MPs were derived from A549 cells). Drug-packaging MPs were characterized from several aspects, including size, plasma membrane origin, mitochondrial and genomic DNA fragments, drug concentration, stability and sterility (Supplementary information, Figures S2 and S3). In addition, using peripheral blood mononuclear cells (PBMCs) from normal donors, we confirmed that such MPs could be taken up by macrophages, monocytes and dendritic cells (DCs); NK cells, T cells and B cells weakly took up MPs (Supplementary information, Figure S4). After a 7-day treatment, > 95% tumor cells in the malignant fluids disappeared (Figure 1A and 1B). In these treated cancer patients, not only the cancer cells in the malignant fluids were eliminated but also the volume, color and turbidity of malignant fluids and symptoms of patients were much ameliorated (Supplementary information, Table S1). However, intrathoracic injection of Cis did not show tumor-killing effect in the other three patients (Figure 1C). These clinical data implicate that the MP-mediated drug delivery system probably possesses the ability to reverse the drug resistance of tumor cells, including Cis resistance, which typically occurs after rounds of chemotherapy. Mounting evidence has demonstrated that epithelial tumor cells acquire stem cell-like features after the epithelial-mesenchymal transition (EMT) [22]. By adapting the previously reported soft 3D fibrin gel method [16], about 1 250 suspending tumor cells isolated from patient's pleural effusion fluids were mixed with 125 μl fibrinogen solution (2 mg/ml fibrinogen, activated by 0.5 units of thrombin). Such fibrin gels correspond to 90 Pa in elastic stiffness [16]. The cells were trapped individually in the 3D fibrin gel and the gel was maintained in a DMEM cell culture medium containing 10% fetal bovine serum (FBS). Inside the soft fibrin gel (90 Pa), those suspending tumor cells indeed could form spheroids (Figure 1D), and the spheroid numbers varied from 210 to 350 (1 250 tumor cells were originally seeded). Based on these clinical results, we hypothesized that treatment with conventional chemotherapeutic drugs induces TRC drug resistance but che-

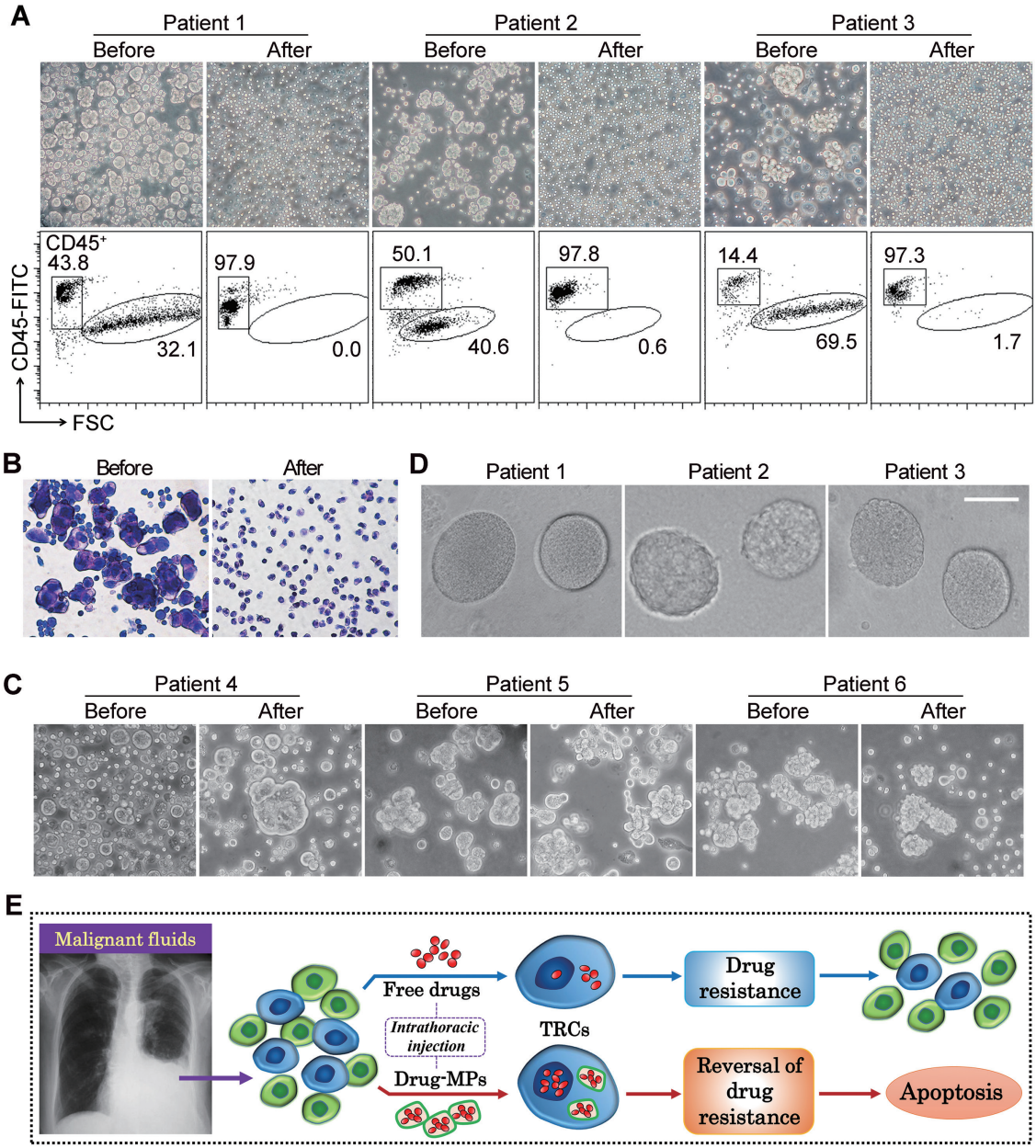


**Figure 1** Drug-packaging MPs target TRCs in cancer patients with malignant pleural effusion. **(A)** Malignant pleural effusion fluids from three end-stage lung cancer patients were collected before and after one-week treatment with intrathoracic injection of Cis-MP. A part of cells harvested from the fluids were smeared on glass slides and observed under microscope (magnification = 200×). A part of cells were stained with FITC-labeled anti-CD45 antibody and analyzed with flow cytometry. **(B)** Cytologic analysis of pleural effusion. The cells in pleural effusion fluids were collected and smeared on glass slides. HE staining showed abundant aggregates of neoplastic cells with conspicuous nucleoli and scanty cytoplasm (magnification = 200×) before treatment. After one-week treatment, most tumor cells in the malignant fluids disappeared and abundant small immune cells were left. **(C)** Malignant pleural effusion fluids from three end-stage lung cancer patients were collected before and after treatment with intrathoracic injection of free Cis for one week. The pleural effusion cells were smeared on glass slides and observed under microscope (magnification = 200×). **(D)** Formation of spheroids of primary tumor cells cultured in 3D soft fibrin gels. $CD45^-$ tumor cells were collected from the pleural effusion fluids and seeded in soft 3D fibrin gels (1 mg/ml, gel stiffness = 90 Pa). Five days later, the spheroids were observed under microscope. Scale bar, 50 μm. **(E)** Treatment with conventional chemotherapeutic drugs induces TRC drug resistance; however, treatment with chemotherapeutic drug-packaging MPs reverses TRC drug resistance in cancer patients with malignant pleural effusions. See also Supplementary information, Figures S1-S4 and Table S1.

motherapeutic drug-packaging MPs might reverse TRC drug resistance in cancer patients with malignant pleural effusion (Figure 1E). We then tested this hypothesis.

Treatment with different concentrations of Cis caused a higher level of cell death in murine H22 hepatocarcinoma cells than in H22 TRCs, indicating that TRCs are more resistant to Cis treatment, consistent with previous findings [16]. Intriguingly, administration of Cis-MPs induced much higher levels of death in TRCs than in parental tumor cells (Figure 2A). Similar results were observed with other chemotherapeutic drugs such as methotrexate (MTX) and DOX (Figure 2A), as well as in TRCs from different cancer cell lines, including human breast cancer MCF-7 and human lung cancer A549 cells (Supplementary information, Figure S5A). More convincingly, the reversal of TRC drug resistance was also confirmed by IC50 assay (Figure 2B). The pan-caspase inhibitor z-VAD-FMK could block the above TRC death (Figure 2C). To exclude the possibility that such apoptosis is due to the mechanical oppression of TRCs by T-MPs, we treated tumor cells with Cis-MPs or MTX-MPs under continuous shaking. TRC apoptosis was consistently observed (Supplementary information, Figure S5B). In addition, when using different amounts of drug-free MPs to treat tumor cells, we did not observe the induction of tumor cell apoptosis (Supplementary information, Figure S5C). MCF-7 and A549 TRCs used in the study exhibited SCLCC features as subcutaneous injection of 100 corresponding TRCs resulted in efficient tumor formation in NOD-SCID mice (5/12 and 4/12 for MCF-7 and A549 TRCs, respectively, versus 0/12 in control mice), consistent with what we have previously reported for human A2780 ovarian cancer TRCs in nude mice [16]. Real-time PCR analysis revealed that the expression of stem cell markers (*Nanog*, *Oct-4* and *Bmi-1*) in MCF-7 TRCs was upregulated compared with that in

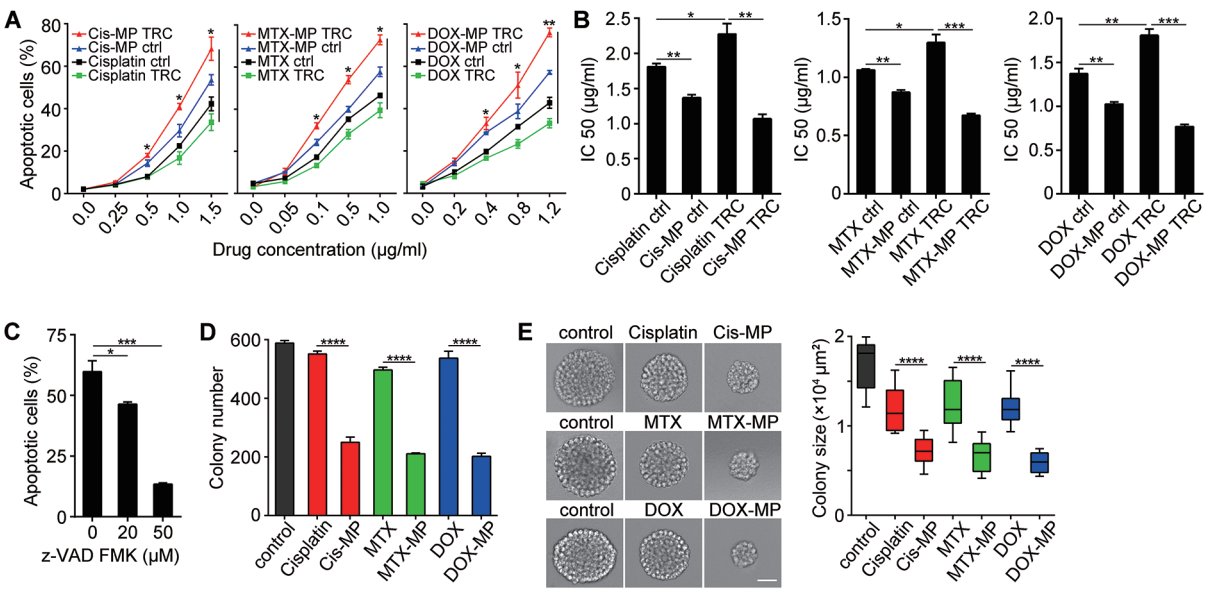


**Figure 2** Drug-packaging MPs could reverse H22 TRC drug resistance *in vitro*. **(A)** H22 hepatocarcinoma tumor cells cultured on conventional rigid plates (control cells) and H22 TRCs ($5 \times 10^4$) were treated with different concentrations of Cis and Cis-MP for 36 h, MTX and MTX-MP for 24 h or DOX and DOX-MP for 36 h. Drug-packaging MPs used in the drug-MP group contained a similar dose of drugs compared with the corresponding free drug group. Then the cells were collected and stained with APC-conjugated Annexin-V for apoptotic detection by flow cytometry. **(B)** The reversal of TRC drug resistance was estimated by the IC50 assay. H22 tumor cells cultured on conventional rigid plates and H22 TRCs ($5 \times 10^3$) were seeded into 96-well plates. Different concentrations of free drug or drug-MPs were added to the experimental group. 24 or 36 h later, the cells were collected and subjected to the MTT assay. **(C)** Drug-packaging MP-induced cell death is dependent on the caspase pathway. H22 TRCs were pre-treated with the pan-caspase inhibitor z-VAD-FMK for 30 min. All groups were then treated with MTX-MP for 20 h and the cells were collected and stained with APC-conjugated Annexin-V for apoptotic detection by flow cytometry. **(D-E)** Analysis of multicellular tumor spheroid (round colony) number and colony size in soft 3D fibrin gels. H22 tumor cells were pre-treated with free drugs (Cis or MTX) or drug-MPs (Cis-MP or MTX-MP) for 4 h. The cells ($n$ = 2 500) from each group were seeded into soft 3D fibrin gels. Five days later, tumor spheroid number **(D)** and colony size **(E)** were calculated. Scale bar, 50 μm. For all graphs, data represent mean ± SEM; $n$ = 3 independent experiments. *$P$ < 0.05, **$P$ < 0.01, ***$P$ < 0.001, ****$P$ < 0.0001 (Student's $t$-test). See also Supplementary information, Figure S5.

control MCF-7 cells (Supplementary information, Figure S5D). We also found a higher proportion of $CD44^+CD24^-$ cells in MCF-7 TRCs versus control cells (Supplementary information, Figure S5E). As expected, MCF-7 TRCs were more drug-resistant than their counterparts from conventional rigid plate culture, and showed a much higher percentage of side population cells in flow cytometric analysis (Supplementary information, Figure S5F), suggesting their stem cell-like nature [23]. On the other hand, a 4-h pretreatment with Cis-MPs, but not with Cis, resulted in much less H22 spheroid formation in soft 3D fibrin gels ($n$ = 250) compared with the control group without the pretreatment ($n$ = 600; Figure 2D). Similar results were obtained when MTX-MPs or DOX-MPs were used (Figure 2D). Besides, colony sizes decreased markedly in the drug-packaging MP treatment group (Figure 2E). ADR/MCF-7 is a highly drug-resistant tumor cell line selected from MCF-7 cells. Like MCF-7, ADR/MCF-7 tumor cells as well as their TRCs were also efficiently targeted by DOX-MPs (Supplementary information, Figure S5G). Together, these data suggest that drug-packaging MPs are capable of partially reversing the drug resistance of TRCs.

*Efficient uptake of drug-packaging MPs by TRCs is due to their softness and deformability*

Drug resistance may result from decrease in drug uptake, increase in drug efflux, inactivation/detoxification of drugs, and the dysregulation of apoptotic pathways [3, 24, 25]. To elucidate how MPs reverse TRC drug resistance, we first examined the uptake of MPs by tumor cells. Surprisingly, when PKH26-labeled MPs were incubated with H22 TRCs or parental cells, ~40% of H22 TRCs versus ~22% of control cells were found to take up MPs (Figure 3A). Such unusual ability to take up T-MPs was also found in Lewis, MCF-7 or A549 TRCs (Figure 3A). The cell cortex (plasma membrane plus the cortical cytoskeleton) deformability could be an important parameter that influences MP uptake, and recent studies have demonstrated that stem cells are more deformable than their differentiated counterparts [26]. We previously showed that B16 melanoma TRCs were several fold softer than differentiated B16 cells [16]. Here, we further found that MCF-7 and A549 TRCs were also much softer than their differentiated counterparts on various substrate rigidities (Figure 3B). We were not able to measure the softness of H22 TRCs due to their suspension growth and the technical difficulties in measuring the softness of suspending cells. When differentiated tumor cells were treated with blebbistatin, a specific inhibitor of non-muscle myosin II contractility that can increase cell softness, an increased uptake of MPs was observed (Figure 3C). Jasplakinolide, a macrocyclic peptide, can decrease cell softness by inducing actin polymerization [27]. When we treated TRCs with jasplakinolide to increase their stiffness, a decreased uptake of MPs was observed (Figure 3D). In addition, MPs seemed to enter the cytoplasm of tumor cells in an intact form (Supplementary information, Figure S6), further supporting the above results. Together, these data suggest that TRCs can efficiently take up membrane-enclosed, drug-packaging MPs because of their relatively high deformability, consistent with the published result that a high ratio of cell softness to particle softness facilitates phagocytosis of MPs [28].

*T-MPs facilitate the retention of drugs in TRCs*

Following the delivery of drugs by T-MPs into TRCs, the retention of drugs in TRCs was further investigated. When cells were treated with DOX, a natural red fluorescent drug, much less DOX was detected in H22 or MCF-7 TRCs than in control tumor cells. However, treatment with drug-packaging MPs resulted in enhanced DOX retention in TRCs compared with DOX treatment, as detected by both flow cytometry and confocal microscopy (Figure 4A and Supplementary information, S7A). Similar results were obtained when tumor cells were treated with DOX-MPs for prolonged time under continuous shaking (Supplementary information, Figure S7B). These data imply that MPs facilitate the retention of drugs in TRCs. Drug efflux is an inverse process of drug retention. In line with the above observations, we found that H22 TRCs showed an increased DOX efflux compared with control H22 cells (Figure 4B). However, this high drug efflux of TRCs was reversed by the pretreatment with drug-free MPs (Figure 4B). Consistently, a similar result was obtained from FITC-dexamethasone-packaging MPs (Supplementary information, Figure S7C). Since we used drug-free medium to refresh the culture medium, the results of Figure 4B should reflect the drug retention rather than uptake of drugs from the medium. Moreover, inhibition of drug efflux should result in fewer drugs in the supernatants. Indeed, HPLC analysis revealed a much lower drug concentration in the supernatants collected from the MP-pretreated (pre-MP) group compared with the control group (Figure 4C and Supplementary information, S7D). Consistently, when supernatants from each group were used to incubate with the same number of tumor cells, tumor cells treated with supernatants harvested from the pre-MP group showed much less DOX fluorescence (Supplementary information, Figure S7E). Furthermore, we observed the appearance of a circle of red DOX around cellular plasma membrane when MCF-7 TRCs were treated with DOX, whereas the peri-plasma membrane drugs disappeared in MP-pretreated cells (Figure 4D), corroborating the ability of MPs to inhibit drug efflux. ADR/MCF-7, the highly

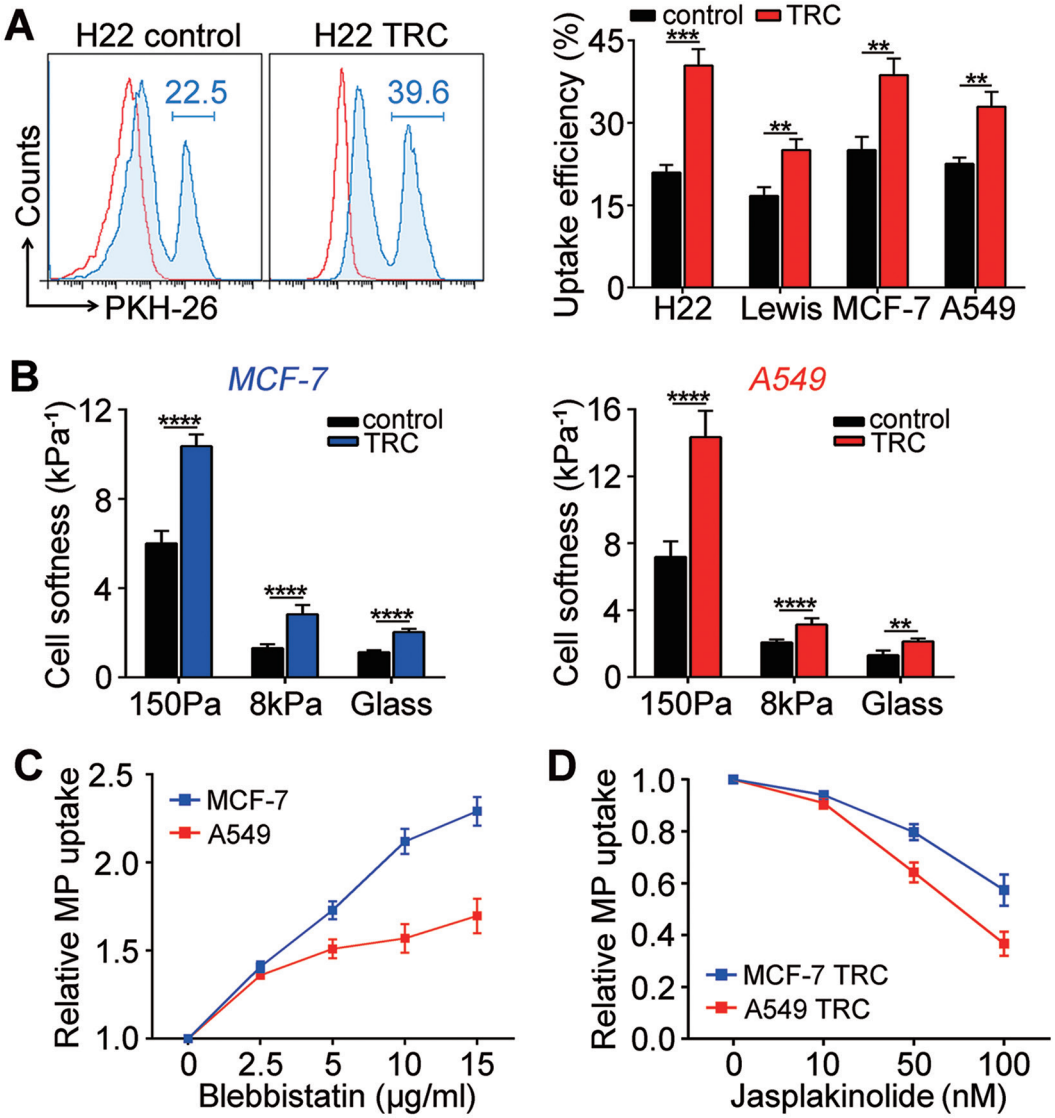


**Figure 3** Soft TRCs efficiently take up drug-packaging MPs. **(A)** Comparison of the abilities of H22 cells and their TRCs to take up T-MPs. PKH26-labeled H22-MPs were incubated with TRCs or control tumor cells (MP/cell = 5 : 1) for 4 h and PKH26-positive cells were detected by flow cytometry (left). The uptake efficiency of different cancer cell lines (H22, Lewis, MCF-7 and A549) and their TRCs was indicated (right). **(B)** MCF-7 and A549 TRCs were more deformable than their differentiated counterparts. Cells were bound with magnetic microbeads and their deformability was measured under an oscillatory magnetic field. $n$ = 3 independent experiments (at least 150 cells per experiment). **(C)** Blebbistatin treatment increased the uptake of MPs. MCF-7 or A549 cells cultured on conventional rigid plates were treated with different concentrations of blebbistatin for 6 h and incubated with PKH26-MPs for 4 h. The cells were then collected and analyzed by flow cytometry. **(D)** Jasplakinolide treatment decreased the uptake of MPs. MCF-7 or A549 TRCs were treated with different concentrations of jasplakinolide for 12 h and incubated with PKH26-MPs for 4 h. The cells were then collected and analyzed by flow cytometry. For all graphs, data represent mean ± SEM; $n$ = 3 independent experiments. *$P$ < 0.05, **$P$ < 0.01, ***$P$ < 0.001, ****$P$ < 0.0001 (Student's $t$-test). See also Supplementary information, Figure S6.

drug-resistant tumor cell line, markedly expressed multidrug-resistant protein P-glycoprotein (P-gp). No co-localization of P-gp and MPs was observed under confocal microscope (Supplementary information, Figure S7F). By contrast, MP treatment downregulated the expression of *ABCB1* (P-gp) in ADR/MCF-7 cells (Figure 4E and 4F). Consistently, the expression of *ABCB1* in MCF-7 TRCs was also decreased by MP treatment (Figure 4G). In addition, we used MPs to treat primary tumor cells from patient's malignant fluids. The results showed that

the expression of *ABC* transporters in these primary cells was downregulated by the MP treatment (Supplementary information, Figure S7G). Taken together, these data may partially explain how MPs hinder drug efflux.

### *MPs facilitate the entry of drugs into the nucleus of TRCs*

Although drug-packaging MPs maintained their integrity in the cytoplasm of TRCs for a period of time, they were eventually ruptured in the cell and released the packaged drugs. To trace the fate of the membranes of MPs that entered the cell, we analyzed various organelles by their trackers. Under confocal microscope, we did not observe any co-localization between MP membranes and mitochondria, endoplasmic reticulum (ER) or Golgi apparatus (Figure 5A). However, we observed high levels of co-localization between MP membranes and lysosomes (Figure 5A). To further dissect out the relationships among MPs, drugs and lysosomes, we examined the distribution of the Lyso-tracker and DOX-MPs in MCF-7 TRCs. Red-fluorescent DOX distributed in both the cytoplasm and nucleus and merged with the Lyso-tracker in the cytoplasm (Supplementary information, Figure S8A). Furthermore, when DOX-packaging, PKH67-labeled MPs were used to treat TRCs, red DOX appeared in the nucleus and co-localized with MP membranes in the cytoplasm (Supplementary information, Figure S8B). On the other hand, we found that inhibition of lysosome enzymes did not influence the apoptosis of TRCs induced by drug-packaging MPs (Supplementary information, Figure S8C). Together, these results suggest that lysosomes play important roles in taking up the MPs, which might be involved in the entry of drugs to the nucleus.

Nuclear entry is a key step for DNA-targeting chemotherapeutic drugs. Since the drugs were distributed inside the nucleus, we tested whether MPs facilitated the entry of drugs into the nucleus. Treatment with conventional dosages of DOX resulted in the entry of only small amounts of the drugs into the nucleus of MCF-7 TRCs. In contrast, after the treatment with drug-packaging MPs, large amounts of the DOX were found in the nucleus

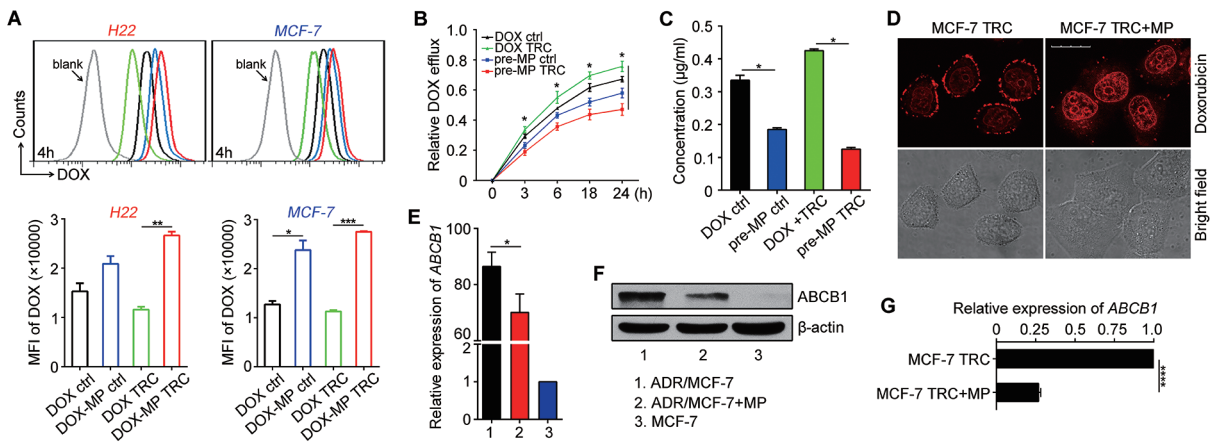


**Figure 4** MPs inhibit drug efflux and increase drug retention in TRCs. **(A)** DOX-MP treatment resulted in enhanced DOX retention in TRCs compared with DOX treatment. H22, MCF-7 TRCs or their control counterparts were incubated with free DOX (1.2 μg/ml) or 1.5 × $10^6$ DOX-MPs (with 1.2 μg/ml DOX) for 4 h and then were incubated in fresh culture medium for additional 6 h. The drug retention was measured by flow cytometric analysis of mean fluorescent intensity (MFI) of DOX. **(B-D)** MP pretreatment inhibited the drug efflux in TRCs. H22 **(B, C)** or MCF **(D)** TRCs or control cells were pretreated with drug-free MPs for 12 h, and then treated with 1 μg/ml DOX for 4 h. After refreshing the culture medium, cells were subjected to various assays as listed in **B-D**. In **B**, cells were further cultured and analyzed by flow cytometry at different time points (0, 3, 6, 18 and 24 h). Differences between MFI measured at the end of the 4-h DOX treatment versus MFI measured at different time points were plotted as the efflux rate. In **C**, cells were further incubated in fresh culture medium for 24 h and supernatants were collected to measure the concentrations of free drugs by HPLC. In **D**, MCF-7 TRCs were observed under two-photon confocal microscope. Scale bar, 20 μm. **(E, F)** MP treatment downregulates *ABCB1* expression in ADR/MCF-7 cells. ADR/MCF-7 cells were treated with MPs for 12 h **(E)** or 48 h **(F)**. The expression of *ABCB1* was analyzed by real-time PCR **(E)** and western blot **(F)**. **(G)** MP treatment downregulates *ABCB1* expression in MCF-7 TRCs. MCF-7 TRCs were treated with or without MPs for 12 h. The expression of *ABCB1* was analyzed by real-time PCR. For all graphs, data represent mean ± SEM; $n = 3$ independent experiments. $^*P < 0.05$, $^{**}P < 0.01$, $^{***}P < 0.001$ (Student's *t*-test). See also Supplementary information, Figure S7.

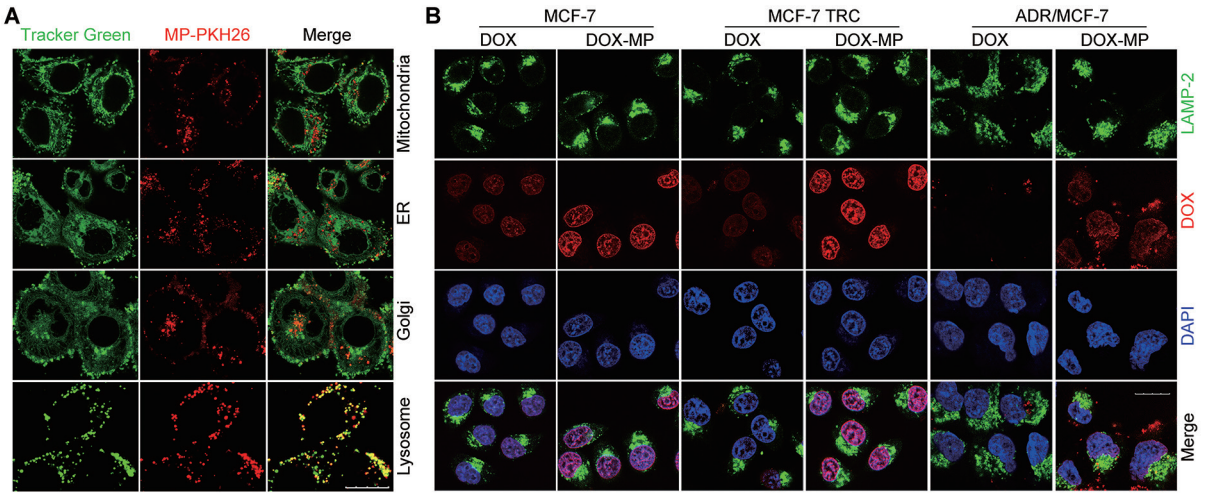


**Figure 5** Drug-packaging MPs facilitate the entry of DOX into the nucleus. **(A)** MP membranes were not present in mitochondria, ER or Golgi apparatus, but showed enhanced co-localization with lysosomes in MCF-7 TRCs. MCF-7 TRCs were incubated with PKH26-labeled MPs for 12 h, and then analyzed with mitochondria, ER, Golgi and lysosome Green Trackers under two-photon confocal microscope. Scale bar, 20 μm. **(B)** MCF-7 cells, MCF-7 TRCs or ADR/MCF-7 cells were treated with DOX (1.2 μg/ml) or 1.5 × $10^6$ DOX-MP (with 1.2 μg/ml DOX) for 12 h, stained with LAMP-2 antibody (green; a lysosomal marker) and DAPI (blue), and observed under two-photon confocal microscope. Scale bar, 20 μm. See also Supplementary information, Figures S8-S10.

(Figure 5B). In addition, pretreatment of cells with drug-free MPs also increased the amount of DOX entering the nucleus (Supplementary information, Figure S9A). Elevating DOX concentration promoted DOX entry into the nucleus, which was further enhanced by the MP pretreatment (Supplementary information, Figure S9B). In clinic, drug-resistant tumor cells can effectively prevent drug entry into the cytoplasm, not to mention drug entry into the nucleus. Even using the ADR/MCF-7 cell line, which is highly resistant to DOX entry, MP pretreatment was highly effective in promoting DOX entry into the nucleus (Supplementary information, Figure S9A). Moreover, like what was observed in MCF-7 TRCs, MPs also delivered DOX to the nucleus of ADR/MCF-7 cells and their TRCs (Figure 5B and Supplementary information, Figure S10).

*Microtubules are involved in MP-mediated entry of drugs into the nucleus of TRCs*

Nuclear envelope alteration might affect the drug entry into the nucleus. Centrosomes have long been known to interact with nuclear envelopes [29]. Confocal microscopy, however, did not show co-localization between centrosomes and PKH67-labeled T-MPs (Supplementary information, Figure S11A), suggesting that centrosome might not have a role in MP-mediated drug entry into the nucleus. Microtubules play important roles in nuclear import [30, 31]. PTX can stabilize microtubule polymerization. To avoid its potential influence on MP uptake by TRCs, we pretreated TRCs with drug-free MPs before addition of PTX. Following the 6-h PTX treatment, DOX was added. The results showed that PTX enhanced MP-induced DOX entry into nuclei (Figure 6A). Furthermore, co-localization between T-MP and β-tubulin was found (Figure 6B and Supplementary information, Figure S11B), and much enhanced co-localization between LAMP-2 and β-tubulin was observed in MP-treated TRCs (Figure 6C and Supplementary information, Figure S11B), suggesting that microtubules are involved in MP-mediated entry of drugs into the nucleus. Dynein is a motor protein on microtubules that mediates the retrograde translocation of vesicles/molecules towards the nucleus [32]. We found that dynein knockdown effectively blocked the entry of DOX into the nucleus (Figure 6D and 6E). Consistently, non-specific dynein inhibitor $Na_3VO_4$ also blocked the entry of DOX into the nucleus (Supplementary information, Figure S11C), but did not affect the cytoplasmic uptake of DOX by cells (Supplementary information, Figure S11D). Together, these data suggest that microtubules are involved in MP-mediated entry of drugs into the nucleus of TRCs.

*Chemotherapeutic drug-packaging MPs reverse TRC drug resistance and prolong the survival of tumor-bearing mice*

To validate the effectiveness of MPs in overcoming

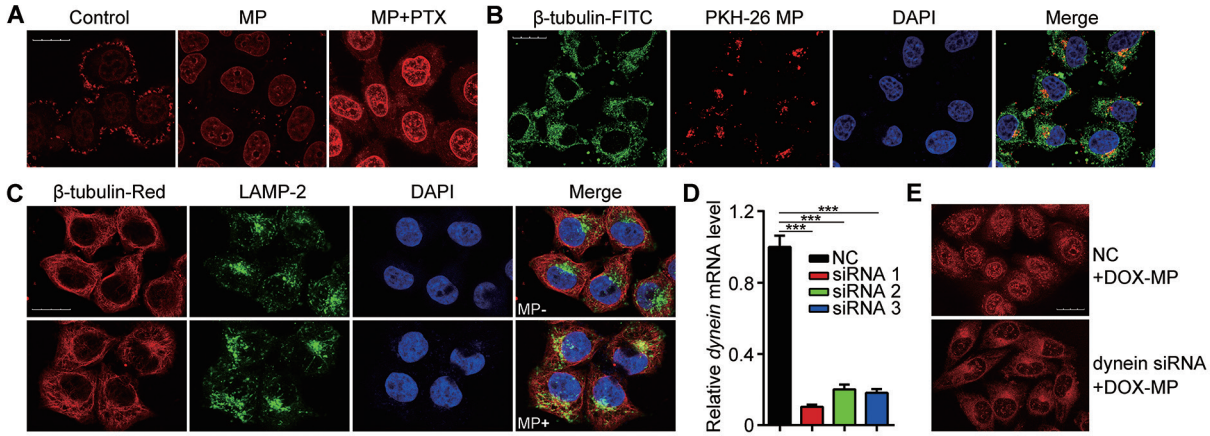


**Figure 6** Microtubules are involved in MP-mediated entry of drugs into the nucleus of TRCs. **(A)** PTX can enhance MP-induced drug entry into nuclei. MCF-7 cells with or without the 12-h MP pretreatment were treated with PTX (6 μg/ml) for 6 h. The cells were then treated with 1 μg/ml DOX for 4 h and observed under two-photon confocal microscope. **(B)** MPs co-localize with β -tubulin in MCF-7 TRCs. PKH26-labeled MPs were incubated with MCF-7 TRCs for 12 h. Then the cells were stained with FITC-labeled anti-β -tubulin antibody (green). DAPI was used to stain the cell nuclei (blue). **(C)** Much enhanced co-localization between LAMP-2 and β -tubulin in MP-treated MCF-7 TRCs. MCF-7 TRCs were incubated with MPs for 12 h. Then the cells were stained with fluorescence-labeled anti-LAMP-2 (green) and anti-β -tubulin (red) antibodies. DAPI was used to stain the cell nuclei (blue). **(D)** Efficiency of Dynein knockdown by siRNAs. Dynein siRNAs or control siRNA (NC) were transfected into MCF-7 TRCs. Twenty-four hours later, the expression of dynein was analyzed by real-time PCR. Error bars indicate mean ± SEM; $n = 3$ independent experiments. ***$P < 0.001$ (Student's *t*-test). **(E)** Dynein knockdown effectively blocked the entry of DOX into the nucleus. Dynein siRNA#1 or control siRNA were transfected into MCF-7 TRCs. Twenty-four hours later, MCF-7 TRCs were incubated with DOX-MPs for 12 h and then observed under two-photon confocal microscope. For all graphs, scale bars indicate 20 μm. See also Supplementary information, Figure S11.

drug resistance *in vivo*, we tested whether drug-packaging MPs were capable of killing TRCs in mice bearing malignant ascites. H22 tumor cells ($5 \times 10^4$) were intraperitoneally (i.p.) injected into BABL/c mice. The next day, Cis-MPs or MTX-MPs ($2 \times 10^6$) were i.p. injected into the mice once every day for 10 days. On day 11, the malignant ascites were collected to count the number of tumor cells by flow cytometry. Compared with MPs or free drugs, injection of Cis-MPs or MTX-MPs significantly reduced the number of $CD45^-$ tumor cells in ascites (Figure 7A), and prolonged the survival of the mice (Figure 7B). Then, 2 500 tumor cells isolated from the ascites were seeded in soft 3D fibrin gels and incubated for 5 days. Much fewer colonies were formed in Cis-MP and MTX-MP groups, compared with control groups (Figure 7C), suggesting that TRCs in malignant ascites were killed by drug-packaging MPs. We also tested the Lewis lung carcinoma-bearing C57BL/6 mouse model. Lewis tumor cells ($8 \times 10^5$) were intravenously (i.v.) injected into C57BL/6 mice to form lung carcinoma. Twenty-four hours later, $2 \times 10^6$ MTX-MPs were i.v. injected into the mice once every day for 10 days. On day 11, some mice were sacrificed for tumor examination and others were maintained for survival analysis. MTX-MP treatment led to reduced number of tumors formed in the lung, compared with the control and MTX-treated groups (Figure 7D). The HE staining also revealed less malignancy in the MTX-MP group (Figure 7E). Tumor cells dissected from lung tissues were seeded in soft 3D fibrin gels. Consistently, MTX-MP treatment, but not MTX treatment, significantly decreased the number of spheroids (Figure 7F). Also, mice receiving MTX-MP treatment had much longer survival time, compared with control and MTX-treated mice (Figure 7G).

To track the distribution pattern of MPs in mice, we injected PKH67-labeled MPs into the above-mentioned mice. In both models, MPs could be detected in the liver, spleen and lung with the peak accumulation achieved 12 h after the injection (Supplementary information, Figures S12A and S13A). We also examined the urine and feces samples from H22 malignant ascite-bearing mice, but did not find the presence of MPs (Supplementary information, Figure S12B). Finally, we measured the drug concentration in various organs and tumor tissues 0.5-48 h after the injection of MTX-MPs ($2 \times 10^6$) into mice via the tail vein. However, HPLC analysis failed to detect the presence of the drugs in these tissues (Supplementary information, Figure S13B), probably due to the low

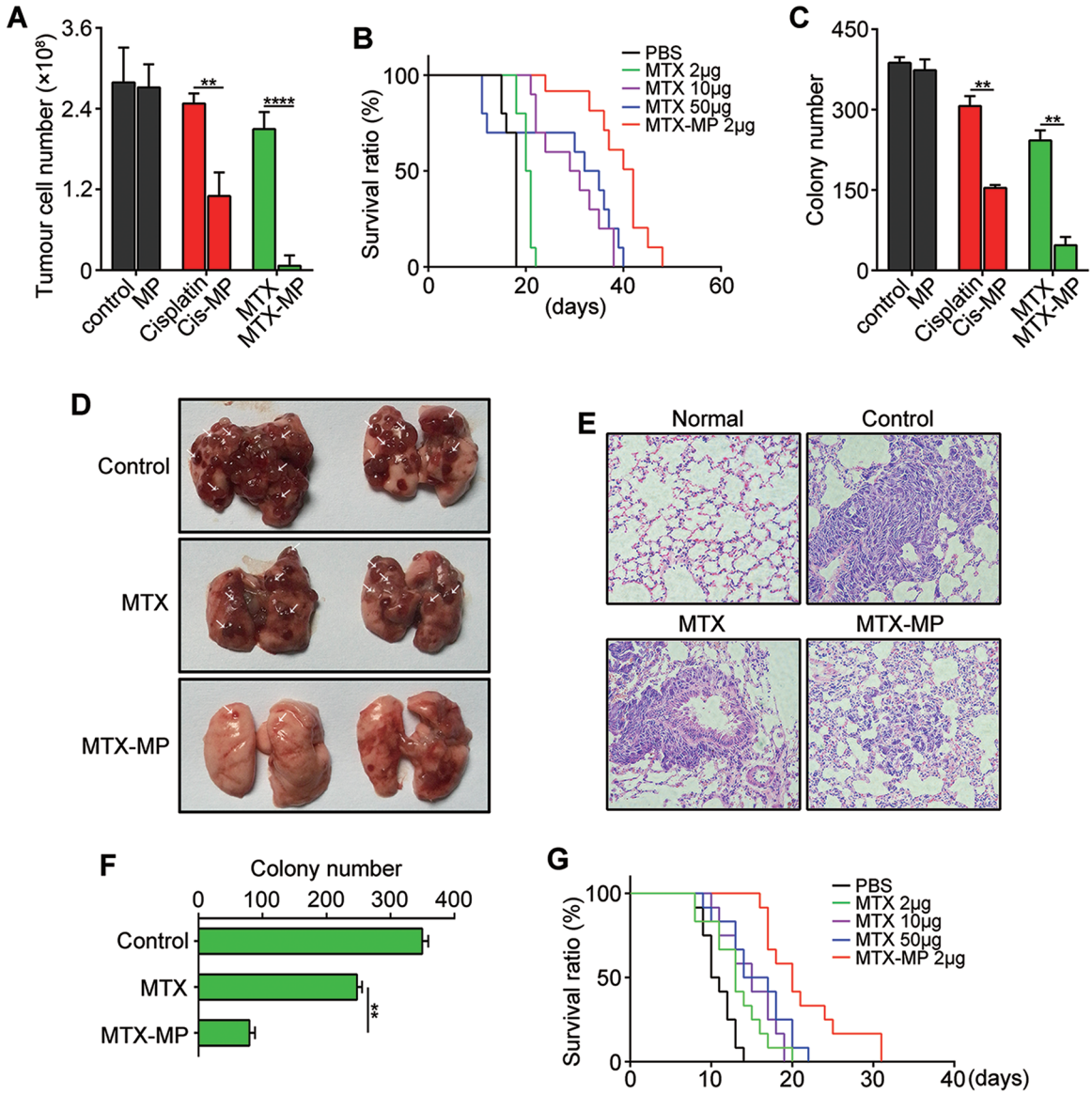


**Figure 7** Drug-packaging MPs effectively target TRCs *in vivo*. **(A)** Drug-packaging MPs effectively kill TRCs in mice bearing H22 malignant ascites. 5 × $10^4$ H22 tumor cells were intraperitoneally (i.p.) injected into BABL/c mice. The next day, 2 × $10^6$ Cis-MPs (containing ~2 μg Cis) or MTX-MPs (containing ~2 μg MTX) were i.p. injected into the mice once every day for 10 days. On day 11, mice were sacrificed and ascites were collected to count the number of $CD45^-$ tumor cells by flow cytometry. **(B)** 5 × $10^4$ H22 tumor cells were i.p. injected into BABL/c mice. The next day, different concentrations of MTX (2, 10, 50 μg) or 2 × $10^6$ MTX-MPs (containing ~2 μg MTX) were i.p. injected into the tumor-bearing mice once every day for 10 days . The long-term survival of tumor-bearing mice was assessed ($n$ = 10). **(C)** Primary tumor cells ($n$ = 2 500) from each group were seeded in soft 3D fibrin gels and incubated for 5 days. The number of tumor spheroids was counted. **(D-F)** Drug-packaging MPs were capable of killing TRCs in the Lewis lung carcinoma-bearing C57BL/6 mouse model. 8 × $10^5$ Lewis tumor cells were intravenously (i.v.) injected into C57BL/6 mice. Twenty-four hours later, MTX (2 μg) or 2 × $10^6$ MTX-MPs (containing ~2 μg MTX) were i.v. injected into the mice once every day for 10 days. On day 11, mice were sacrificed and the tumors were indicated by the white arrow **(D)** and confirmed by HE staining **(E)**. The isolated tumor cells were seeded in soft 3D fibrin gels. The tumor spheroid number was counted **(F)**. For all graphs, data represent mean ± SEM; $n$ = 3 independent experiments. $^{**}P < 0.01$, $^{****}P < 0.0001$ (Student's $t$-test). **(G)** 8 × $10^5$ Lewis tumor cells were i.v. injected into C57BL/6 mice. Twenty-four hours later, different concentrations of MTX (2, 10, 50 μg) and 2 × $10^6$ MTX-MPs (with ~2 μg MTX) were i.v. injected into the tumor-bearing mice once every day for 10 days. The long-term survival of tumor-bearing mice was assessed by the Kaplan-Meier method ($n$ = 12). Data are representative of three independent experiments. $P < 0.0001$; MTX-MP group vs PBS control group. See also Supplementary information, Figures S12 and S13.

quantity of MTX in the MPs.

## Discussion

Although cancer therapies have been greatly improved, drug resistance is still a formidable hurdle [33]. Reversing drug resistance faces two basic challenges, i.e., how to expose tumor cells to sufficiently high local concentration of drugs and how to bring enough drugs into tumor cells to exert their functions. This study clearly shows that T-MP-mediated drug delivery, by virtue of their biological features, can effectively overcome these two barriers by packaging highly concentrated drugs into the MPs and facilitating drug entry into the nucleus of tumor cells.

A surprising finding from our study lies in that TRCs are more effective in taking up T-MPs than their differentiated counterparts due to their softness, indicating that the physical trait may play an important role in tumor cell biology. Previous studies have shown that metastasis appears to occur primarily in soft organs/tissues in cancer patients [34, 35] and cancer cells from metastatic tumors were softer [36]. Although the underlying mechanisms are not fully understood, we have recently proposed a putative model, in which cell and tissue softness contributes to the tropism of cancer metastasis and recurrence [17]. Here, we provide further evidence that the soft feature of the cell renders TRCs to effectively take up the MPs. We demonstrate that TRCs from different tumor types, both human and mouse, are softer than the differentiated tumor cells. Soft TRCs can easily undergo deformation and thus efficiently take up MPs. Although we identify that cellular softness is involved in T-MP uptake by TRCs, it remains unclear how T-MPs cross the membrane and enter the cytoplasm of TRCs. Our unpublished data revealed that T-MPs were taken up by macrophages or DCs via endocytosis/phagocytosis pathway. In these immune cells, there was very clear co-localization between T-MPs and early endosomes, later endosomes and lysosomes. By contrast, we found that T-MPs did not co-localize with early or late endosomes in TRCs. In addition, treatment with EIPA, an inhibitor of the macropinocytosis pathway, almost completely blocked the uptake of dextran (positive control), but did not affect T-MP uptake by TRCs (data not shown). Therefore, uptake of T-MPs by TRCs appears not to be mediated by phagocytosis or macropinocytosis, but through an unknown pathway. After entering the cytoplasm, drug-packaging MPs in turn release drugs, leading to the destruction of TRCs via a Trojan horse-like strategy. More significantly, MPs do not just simply release drugs into the cytoplasm of TRCs but escort drugs into the lysosome and nucleus, subsequently triggering apoptosis of TRCs. Interestingly, although MPs could deliver drugs into lysosomes, inhibition of lysosome enzymes did not influence TRC apoptosis induced by drug-packaging MPs. The significance of MP-mediated drug delivery into lysosomes remains unclear. One possibility is that lysosomes are involved in MP-mediated delivery of drugs into the nucleus. It is interesting to point out that normal acidic lysosomes tend to sequester chemotherapeutic drugs, leading to increasd drug resistance [37]. Dysfunction in lysosomes can result in enhanced drug sensitivity of cancer cells [38, 39]. Vacuolar-type $H^+$-ATPase on the lysosomal membrane pumps protons into the lysosomal lumen and maintains the acidity of lysosome [40]. In addition, the activation of NOX2 on lysosomal membrane causes the production of superoxide, leading to the consumption of protons due to the generation of hydrogen peroxide, thus regulating the pH of lysosomes [41]. Considering the co-localization of MPs and lysosomes, it is possible that the uptake of MPs by lysosomes might influence the activity of $H^+$-ATPase or NOX2, thus regulating the pH and the function of lysosomes. Microtubules are known to play important roles in regulating nuclear import and drug resistance [42]. In this study, we demonstrate that microtubules participate in MP-mediated entry of drugs into the nucleus, and the co-localization of MPs and microtubules indicates the possible interaction between MPs and microtubules. Whether and how lysosomes facilitate the transfer of drugs into the nucleus are worthy of further investigation, which may provide deep mechanistic insights into MP biology and MP-based drug delivery systems.

Based on previous studies and our current findings, we summarize several unique merits possessed by MPs: (i) their membrane structures are resistant to detergents such as Triton X-100, indicating enriched composition of lipid rafts [21]; (ii) physical softness of cells determines their efficiency in taking up MPs; (iii) drug-packaging MPs not only deliver drugs into the nucleus but also are capable of interfering with the ABC transporter system to impede drug efflux pump; (iv) MPs are capable of interacting with lysosomes and/or cytoskeletons. MPs as a natural drug delivery system are much different from synthetic microparticles and possess multiple advantages in cancer therapy: (i) packaging both soluble and insoluble drugs with high efficiency; (ii) possessing considerable volume to package large amounts of drug molecules; (iii) high stability due to their lipid raft-enriched membrane structure; (iv) direct delivery of drugs into tumor cells; (v) delivery of drugs into the nucleus of tumor cells; (vi) safety and absence of toxicity to the body. In addition, the preparation of tumor cell-derived, drug-packaging MPs is simple, further facilitating their

applicability. These features make drug-packaging MPs highly efficacious in targeting tumor cells, especially for stem cell-like TRCs. Consistently, in three Cis-MP-treated cancer patients, not only the cancer cells in the malignant fluids were eliminated but also the volume, color and turbidity of malignant fluids and symptoms of patients were much ameliorated. Such clinical benefits continue to be observed in our ongoing trials. These clinical results suggest that drug-packaging MPs can target TRCs and reverse drug resistance of TRCs in the malignant fluids of cancer patients (Figure 1E). Multiple mechanisms may account for the ability of MPs to reverse TRC drug resistance, i.e., facilitating drug uptake, impeding drug efflux, and promoting drug entry into the nucleus. Although these mechanisms were elucidated from tumor cell lines, they might also be applied to patient TRCs. Different cell types may have different features, but they also share many similarities in basic properties. For example, we found that both murine and human TRCs are physically softer than their differentiated counterparts (Figure 3), enabling TRCs to efficiently take up drug-MPs. Lysosomes are common organelles shared by all cell types. We found that drug-MPs went into lysosomes after entering the cell, and this phenomenon was confirmed in murine H22 hepatocarcinoma, murine B16 melanoma, human MCF-7 breast cancer and human A549 lung cancer cell lines, suggesting that patient TRCs and tumor cell line TRCs may have consistent responses to drug-MPs.

In summary, our study shows that tumor cell-derived MPs packaged with drugs, by virtue of their unique bio-carrier features, can efficiently deliver chemotherapeutic drugs into the nucleus of stem cell-like TRCs, leading to the reversal of drug resistance of TRCs and the killing of TRCs in animal tumor models and in patients. The preferential uptake of drug-packaging MPs by TRCs due to their increased softness is remarkable, suggesting that physical properties of cancer cells might be targeted to overcome drug resistance. Our present study provides a novel strategy to reverse the drug resistance of SCLCCs with potential clinical applications.

## Materials and Methods

*Cell lines and animals*

Murine hepatocarcinoma cell line H22, murine lung carcinoma cell line Lewis, human breast carcinoma cell line MCF-7, DOX-resistant carcinoma cell line ADR/MCF-7 and human lung carcinoma cell line A549 were obtained from China Center for Type Culture Collection (Wuhan, China) and maintained in a rigid dish with RMPI-1640 or DMEM cell culture medium (Invitrogen) supplemented with 10% FBS (Gibco) at 37 °C with 5% $CO_2$. Female BALB/c and C57BL/6 mice (6-8-week old) were purchased from Center of Medical Experimental Animals of Hubei Province (Wuhan, China) for studies approved by the Animal Care and Use Committee of Tongji Medical College.

*Reagents and antibodies*

DOX, MTX, Cis and PTX were purchased from Beijing Huafeng United Technology Co., Ltd. Pan-caspase inhibitor z-VAD-FMK, proteinase inhibitor E-64 and pepstatin A, dynein inhibitor $Na_3VO_4$, PKH26 Red and PKH67 Green Fluorescent Cell Linker Kit were purchased from Sigma. ER-, Mito-, Lyso-tracker Green and CellLight Golgi-GFP were purchased from Invitrogen. The following primary antibodies, anti-LAMP2 (ab25631), anti-β-tubulin (ab15568), anti-centrin1 (ab11257), anti-cytochrome C (ab110325), anti-caspase-3/6/7/9 (ab13847/ab108335/ab25900/ab47537), and anti-histone H2B/H3 (ab1790/ab10812), were purchased from Abcam. Anti-P-glycoprotein antibody (P7965) were purchased from Sigma. Anti-β-actin antibody (ANT009) were purchased from *Ant* Gene. Secondary antibodies, goat anti-mouse IgG FITC, donkey anti-rabbit IgG Alexa Fluor488, and goat anti-rabbit IgG Dylight594, were purchased from Abcam.

*Preparation of drug-packaging MPs*

For the clinical trial, $2.5 \times 10^8$ A549 cells in 20 ml culture media were first exposed to ultraviolet irradiation (UVB, 300 J/$m^2$) for 1 h. 500 μg/ml Cis was then added to the culture medium. 16 h later, supernatants were collected for centrifugation: first 10 min at 600× *g*, and then 2 min at 14 000× *g* to get rid of cell debris. Finally, the supernatants were centrifuged for 60 min at 14 000× *g* to pellet MPs ($2.5 \times 10^7$). The pellets were washed and re-suspended in 0.9% saline for injection once for one patient. The whole process was conducted according to good manufacturing practice (GMP) quality standard. For each preparation, the same amount of drugs treat the same number of tumor cells in the same volume of media with the same treatment time to keep the stability and reproducibility of drug-packaging MPs. The size, drug concentration, and sterility of drug-packaging MPs were characterized in Supplementary information, Figure S3.

*Patients*

This human subject study included 6 end-stage lung cancer patients with metastatic malignant pleural effusion at present or in relapse between 2013 and 2015 at the Union Hospital, Hubei Provincial Hospital of TCM and the Fifth Hospital of Wuhan. The study was approved by the Clinical Trial Ethics Committee of Huazhong University of Science and Technology. All patients have received rounds of chemotherapy, and developed multidrug resistance. All patients have provided written informed consent to participate in the study. Three of them were treated with intrathoracic injection of drug-packaging MPs for 1-4 weeks. The other three patients were treated with intrapleural injection of drug alone. Pleural effusion fluids were obtained from all patients and analyzed in our laboratory. Detailed clinical information of treated patients is described in Supplementary information, Table S1.

*Conventional 2D rigid dish and 3D fibrin gel cell culture of tumor cells*

For conventional 2D cell culture, B16-F1 cells were maintained in rigid dish with MEM cell culture medium supplemented with 10% FBS (Invitrogen, Carlsbad, CA, USA) at 37 °C with 5% $CO_2$. TRC culture was conducted according to the previous method [16]. In brief, tumor cells were maintained in the conventional

rigid plate. After 0.25% trypsin digestion, cells were detached and suspended in DMEM medium (10% FBS) and cell density was adjusted to $10^4$ cells/ml. Fibrinogen (Searun Holdings Company, Freeport, ME, USA) was diluted to 2 mg/ml with T7 buffer (50 mM Tris, pH 7.4, 150 mM NaCl). 1:1 fibrinogen and cell solution mixture was made by mixing the same volume of the fibrinogen solution and the cell solution, resulting in 1 mg/ml fibrinogen and 5 000 cells/ml in the mixture. 250 μl cell/fibrinogen mixtures were seeded into each well of 24-well plate and mixed well with pre-added 5 μl thrombin (0.1 U/μl, Searun Holdings Company). The cell culture plate was then moved to 37 °C cell culture incubator and incubated for 30 min. Finally, 1 ml DMEM medium containing 10% FBS and antibiotics were added. On day 5, the cells cultured in soft 3D fibrin gels (90 Pa) were treated with dispase II (Roche) for 10 min at 37 °C and then the spheroids were harvested and pipetted to single cells.

*MTT assay*

H22 tumor cells cultured on conventional rigid plate and H22 TRCs were seeded in 96-well plates with 100 μl cell culture medium in each well at a concentration of $5 \times 10^4$ cells/ml. Cells were cultured to the logarithmic growth phase and free drugs or drug-MPs were then added to the experimental group with different concentrations. RPMI-1640 cell culture medium was added to the blank control group. The cells were then cultured at 37 °C with 5% $CO_2$ and saturated humidity. Cells were cultured for various times (24 or 36 h). The cells were collected and measured by 3-(4,5-dimethylthiazol-2-yl)-2,5-diphenyl tetrazolium bromide (MTT, Sigma) assay. MTT was prepared as a 5 mg/ml stock solution in PBS, sterilized by Millipore filtration, and kept in darkness. The 50 μl of MTT solution was added into each well without removal of culture medium. After 4 h incubation at 37 °C, 100 μl of dimethyl sulfoxide was added to dissolve the formazan crystals. The dissolvable solution was agitated homogeneously for about 15 min by a shaker. The absorbance (A value) was measured at a wavelength of 570 nm by a microplate reader, with the A value at a wavelength of 620 nm as a reference, and the inhibition rate of the cells was calculated as follows: Inhibition rate (%) = (A value (control group) − A value (test group))/(A value (control group) – A value (blank group)) × 100.

*Quantification of cell softness*

Cell stiffness was measured by applying an oscillatory magnetic field (the applied stress $\sigma = 15.5$ Pa at 0.3 Hz) and measuring the resultant oscillatory bead displacement using published protocols [2]. Cell softness or deformability is the inverse of cell stiffness.

*High-performance liquid chromatography (HPLC)*

The concentration of chemotherapeutic drug in MPs was measured by HPLC. Briefly, A549 tumor cell-derived, Cis-, MTX- and DOX-packaging MPs were processed by the lysis buffer containing proteinase K, phenylmethylsulphonyl fluoride and DNase I. The HPLC system consists of a 1525 Binary HPLC Pump, a 717 Plus Autosampler and a 2475 Multi-Wavelength Fluorescence Detector (Waters Corporation, Milford, CT, USA). Chromatography was performed on a column (4.6 × 150 $mm^2$, particle size 5 mm). The effluents were monitored at an excitation wave length of 480 nm and an emission wave length of 560 nm at 40 °C. Detection and integration of chromatographic peaks was performed using Empower 2 software (Waters Corporation).

*Flow cytometry*

C6 flow cytometer (BD) was used for the flow cytometric analysis of the samples. Drug-packaging MPs were prepared and added to the cultured tumor cells. The cells were collected and stained with FITC-Annexin V and propidium iodide for apoptosis detection by a flow cytometer.

*Real-time PCR*

Real-time PCR analyses were performed with 2 μg of cDNA as a template, using a SYBR Green mix (Applied Bioscience) and an Agilent Technologies Stratagene Mx3500P real-time PCR system. Analysis was performed using Mxpro software (Stratagene) and relative quantification was performed using the ΔΔCt method with GAPDH as a reference. The entire procedure was repeated in at least three biologically independent samples.

*Western blotting*

Whole cell lysates were prepared from ADR/MCF-7 cells and MCF-7 cells and separated by SDS-PAGE at 100 V for 1 h. Separated proteins were then transferred to NC membranes (Millipore, Billerica, MA, USA). The membranes were blocked in 5% BSA in TBS containing 0.1% Tween-20 for 1 h at room temperature. Then the membranes were incubated with anti-P-gp antibody or anti-β-actin antibody overnight at 4 °C. The membranes were washed three times and incubated with HRP-conjugated secondary antibodies. Proteins were visualized by ECL western blotting reagent (Themo Pierce, Rockford, IL, USA).

*Immunofluorescence staining*

All antibodies described earlier were used on frozen sections. Cells were fixed in 4% paraformaldehyde for 10 min at room temperature, permeabilized with 0.3% Triton X-100 and blocked with 1% BSA for 1 h at 25 °C. Samples were incubated with primary antibodies (in PBST and 1% BSA) overnight at 4 °C. Cells were washed three times in PBS and incubated with secondary antibodies for 1 h at room temperature. Nuclei were stained with the DAPI solution (1 μg/ml). Merged figure shows the bright field image and fluorescent image observed under a two-photon fluorescent microscope.

*Gene silencing experiments*

siRNAs targeting human dynein (siRNA#1: GCAAGAATGTCGCTAAATT; siRNA#2: GGATGACAATAAGCTCCTA; siRNA#3: GACCCATCTTGTACAGCAA) and control siRNA were purchased from RiboBio (Guangzhou, China). siRNA (50 nM) was transfected into MCF-7 TRCs using lipofectamine RNAiMax (Invitrogen) according to the manufacturer's instruction.

*Statistics analysis*

All experiments were performed at least three times. Results were expressed as mean ± SEM and analyzed by Student's *t*-test. The *P*-values < 0.05 were considered statistically significant. The analysis was conducted using the Graphpad 6.0 software.

## Acknowledgments

This work was supported by the National Basic Research

Program of China (2014CB542100 and 2012CB932500), the National Science Fund for Distinguished Young Scholars of China (81225021), the National Natural Science Foundation of China (81472653 and 81530080), the Special Fund of Health Public Welfare Profession of China (201302018), and funds from Huazhong University of Science and Technology.

*Author Contributions*

BH conceived the project. JWM, YZ, KT, HFZ, XNY, YL, PWX, YLS, RHM, TTJ, JWC, SZ, TZZ, SQL, XLL, CYL, WHG and ZXL performed the experiments. BH, NW, XLY, ZWH and XTC developed methodology. BH, NW, XLY, ZWH, XTC performed data analysis. JZL provided administrative, technical, or material support. BH, JWM and NW wrote the manuscript with input from all authors.

*Competing Financial Interests*

BH was supported by Soundny (Sheng-Qi-An) Biotech. The remaining authors declare no competing financial interests.

## References

1 Pattabiraman DR, Weinberg RA. Tackling the cancer stem cells — what challenges do they pose? *Nat Rev Drug Discov* 2014; **13**:497-512.
2 Wang Z, Li Y, Ahmad A, *et al.* Targeting miRNAs involved in cancer stem cell and EMT regulation: an emerging concept in overcoming drug resistance. *Drug Resist Updat* 2010; **13**:109-118.
3 Dean M, Fojo T, Bates S. Tumour stem cells and drug resistance. *Nat Rev Cancer* 2005; **5**:275-284.
4 Vermeulen L, de Sousa e Melo F, Richel DJ, Medema JP. The developing cancer stem-cell model: clinical challenges and opportunities. *Lancet Oncol* 2012; **13**:e83-e89.
5 Visvader JE, Lindeman GJ. Cancer stem cells in solid tumours: accumulating evidence and unresolved questions. *Nat Rev Cancer* 2008; **8**:755-768.
6 Fulda S. Regulation of apoptosis pathways in cancer stem cells. *Cancer letters* 2013; **338**:168-173.
7 Blanpain C, Mohrin M, Sotiropoulou PA, Passegue E. DNA-damage response in tissue-specific and cancer stem cells. *Cell Stem Cell* 2011; **8**:16-29.
8 Dean M. ABC transporters, drug resistance, and cancer stem cells. *J Mammary Gland Biol Neoplasia* 2009; **14**:3-9.
9 Roesch A, Fukunaga-Kalabis M, Schmidt EC, *et al.* A temporarily distinct subpopulation of slow-cycling melanoma cells is required for continuous tumor growth. *Cell* 2010; **141**:583-594.
10 Sharma SV, Lee DY, Li B, *et al.* A chromatin-mediated reversible drug-tolerant state in cancer cell subpopulations. *Cell* 2010; **141**:69-80.
11 Haq R, Yokoyama S, Hawryluk EB, *et al.* BCL2A1 is a lineage-specific antiapoptotic melanoma oncogene that confers resistance to BRAF inhibition. *Proc Natl Acad Sci USA* 2013; **110**:4321-4326.
12 Takebe N, Miele L, Harris PJ, *et al.* Targeting Notch, Hedgehog, and Wnt pathways in cancer stem cells: clinical update. *Nat Rev Clin Oncol* 2015; **12**:445-464.
13 Pan Q, Li Q, Liu S, *et al.* Concise review: targeting cancer stem cells using immunologic approaches. *Stem Cells* 2015; **33**:2085-2092.
14 Prasad S, Gaedicke S, Machein M, *et al.* Effective eradication of glioblastoma stem cells by local application of an AC133/CD133-specific T-cell-engaging antibody and CD8 T cells. *Cancer Res* 2015; **75**:2166-2176.
15 Clevers H. The cancer stem cell: premises, promises and challenges. *Nat Med* 2011; **17**:313-319.
16 Liu J, Tan Y, Zhang H, *et al.* Soft fibrin gels promote selection and growth of tumorigenic cells. *Nat Mater* 2012; **11**:734-741.
17 Tan Y, Tajik A, Chen J, *et al.* Matrix softness regulates plasticity of tumour-repopulating cells via H3K9 demethylation and Sox2 expression. *Nat Commun* 2014; **5**:4619.
18 Wolf P. The nature and significance of platelet products in human plasma. *Br J Haematol* 1967; **13**:269-288.
19 Mause SF, Weber C. Microparticles: protagonists of a novel communication network for intercellular information exchange. *Circ Res* 2010; **107**:1047-1057.
20 Zhang Y, Zhang R, Zhang H, *et al.* Microparticles released by Listeria monocytogenes-infected macrophages are required for dendritic cell-elicited protective immunity. *Cell Mol Immunol* 2012; **9**:489-496.
21 Tang K, Zhang Y, Zhang H, *et al.* Delivery of chemotherapeutic drugs in tumour cell-derived microparticles. *Nat Commun* 2012; **3**:1282.
22 Polyak K, Weinberg RA. Transitions between epithelial and mesenchymal states: acquisition of malignant and stem cell traits. *Nat Rev Cancer* 2009; **9**:265-273.
23 Chen L, Xiao Z, Meng Y, *et al.* The enhancement of cancer stem cell properties of MCF-7 cells in 3D collagen scaffolds for modeling of cancer and anti-cancer drugs. *Biomaterials* 2012; **33**:1437-1444.
24 Gottesman MM. Mechanisms of cancer drug resistance. *Annu Rev Med* 2002; **53**:615-627.
25 Baylin SB. Resistance, epigenetics and the cancer ecosystem. *Nat Med* 2011; **17**:288-289.
26 Chowdhury F, Na S, Li D, *et al.* Material properties of the cell dictate stress-induced spreading and differentiation in embryonic stem cells. *Nat Mater* 2010; **9**:82-88.
27 Holzinger A. Jasplakinolide: an actin-specific reagent that promotes actin polymerization. *Methods Mol Biol* 2009; **586**:71-87.
28 Beningo KA, Wang YL. Fc-receptor-mediated phagocytosis is regulated by mechanical properties of the target. *J Cell Sci* 2002; **115**:849-856.
29 Nigg EA, Stearns T. The centrosome cycle: Centriole biogenesis, duplication and inherent asymmetries. *Nat Cell Biol* 2011; **13**:1154-1160.
30 Salman H, Abu-Arish A, Oliel S, *et al.* Nuclear localization signal peptides induce molecular delivery along microtubules. *Biophys J* 2005; **89**:2134-2145.
31 Campbell EM, Hope TJ. Role of the cytoskeleton in nuclear import. *Adv Drug Deliv Rev* 2003; **55**:761-771.
32 Roberts AJ, Kon T, Knight PJ, Sutoh K, Burgess SA. Functions and mechanics of dynein motor proteins. *Nat Rev Mol Cell Biol* 2013; **14**:713-726.
33 Bourzac K. Biology: Three known unknowns. *Nature* 2014; **509**:S69-S71.

34 Valastyan S, Weinberg RA. Tumor metastasis: molecular insights and evolving paradigms. *Cell* 2011; **147**:275-292.
35 Plodinec M, Loparic M, Monnier CA, *et al.* The nanomechanical signature of breast cancer. *Nat Nanotechnol* 2012; **7**:757-765.
36 Cross SE, Jin YS, Rao J, Gimzewski JK. Nanomechanical analysis of cells from cancer patients. *Nat Nanotechnol* 2007; **2**:780-783.
37 Yamagishi T, Sahni S, Sharp DM, Arvind A, Jansson PJ, Richardson DR. P-glycoprotein mediates drug resistance via a novel mechanism involving lysosomal sequestration. *J Biol Chem* 2013; **288**:31761-31771.
38 von Schwarzenberg K, Lajtos T, Simon L, Muller R, Vereb G, Vollmar AM. V-ATPase inhibition overcomes trastuzumab resistance in breast cancer. *Mol Oncol* 2014; **8**:9-19.
39 Zong D, Zielinska-Chomej K, Juntti T, *et al.* Harnessing the lysosome-dependent antitumor activity of phenothiazines in human small cell lung cancer. *Cell Death Dis* 2014; **5**:e1111.
40 Sun-Wada GH, Wada Y. Vacuolar-type proton pump ATPases: acidification and pathological relationships. *Histol Histopathol* 2013; **28**:805-815.
41 Savina A, Jancic C, Hugues S, *et al.* NOX2 controls phagosomal pH to regulate antigen processing during crosspresentation by dendritic cells. *Cell* 2006; **126**:205-218.
42 Orr GA, Verdier-Pinard P, McDaid H, Horwitz SB. Mechanisms of Taxol resistance related to microtubules. *Oncogene* 2003; **22**:7280-7295.

(**Supplementary information** is linked to the online version of the paper on the *Cell Research* website.)